INTERNATIONAL JOURNAL OF INTEGRATED ENGINEERING
ISSN: 2229-838X e-ISSN: 2600-7916

IJIE

Vol. 16 No. 9 (2024) 339-350
https://publisher.uthm.edu.my/ojs/index.php/ijie

# Automated X-Ray Inspection (AXI) on Surface Mount Technology Resistor (SMT-Res) Defects Detection Using GAN-YOLOv8n Model

**Lau Pui Ching[1], A. R. Syafeeza[1]*, Norihan Abdul Hamid[1], Norazlina Abdul Razak[1], Wira Hidayat Mohd Saad[1], Wong Yan Chiew[1], Surinarayanan Prasad[2]**

[1] *Machine Learning & Signal Processing (MLSP) Research Group, Centre for Telecommunication Research and Innovation (CeTRI), Fakulti Teknologi dan Kejuruteraan Elektronik dan Komputer (FTKEK), Universiti Teknikal Malaysia Melaka, 76100 Durian Tunggal, Melaka, MALAYSIA*
[2] *Intel Product's (M) Sdn. Bhd, 12000 Butterworth, Pulau Pinang, MALAYSIA*

*Corresponding Author: syafeeza@utem.edu.my
DOI: https://doi.org/10.30880/ijie.2024.16.09.028

**Article Info**

Received: 18 August 2024
Accepted: 14 September 2024
Available online: 30 December 2024

**Keywords**

YOLO, generative adversarial network, surface mount technology resistor, automated X-ray inspection, deep learning

**Abstract**

Product quality is a crucial factor in the electronic manufacturing sector, with inspection playing a significant role. However, human inspectors' accuracy fluctuates due to factors like fatigue, turnover, experience, and inconsistent fault categorization. These inconsistencies result in longer inspection times and operator-specific quality variations. To address this challenge, AI automation within Industry 4.0 framework is increasingly adopted to replace human involvement and reduce annual costs in quality control and testing. This paper proposes an Automated X-ray Inspection (AXI) system that develops a defects detector framework for detecting and classifying Surface Mount Technology-Resistor (SMT-Res) on PCBs, using a private dataset from Intel Technologies. The YOLOv7 and YOLOv8 models are examined as detectors, and experimental results highlight the exceptional performance of the GAN-YOLOv8n model. With just 3.01M parameters, it achieves 92.9% mean average precision (mAP) at Intersection over Union (IoU) 0.5 and 71.5% mAP at IoU 0.95, demonstrating excellent accuracy and efficiency. The proposed AXI system, leveraging AI automation, offers a promising solution for improving inspection processes, reducing costs, and enhancing product quality in electronic manufacturing.

## 1. Introduction

Artificial Intelligence (AI) has been applied for Printed Circuit Board (PCB) quality control and inspection in recent years. Nowadays, PCB is the most significant component that can be found in almost all electronic products such as electronic gadgets, Internet of Things (IoT) devices, automotive, or even high-end products like medical infrastructure, military weapons, airplane, and satellite.

According to a market research report published in 2020, the global market for PCBs is expected to reach a value of $71.7 billion by 2025, with a compound annual growth rate of 5.4% from 2020 to 2025. The report cites factors such as the increasing demand for electronic devices, the growing adoption of advanced technologies, and the expansion of the IoT as drivers of the PCB market [1]. Fig. 1. shows the PCB manufacturing process. There are 4 stages which consist of printing, mounting, reflow soldering, and inspection and testing.

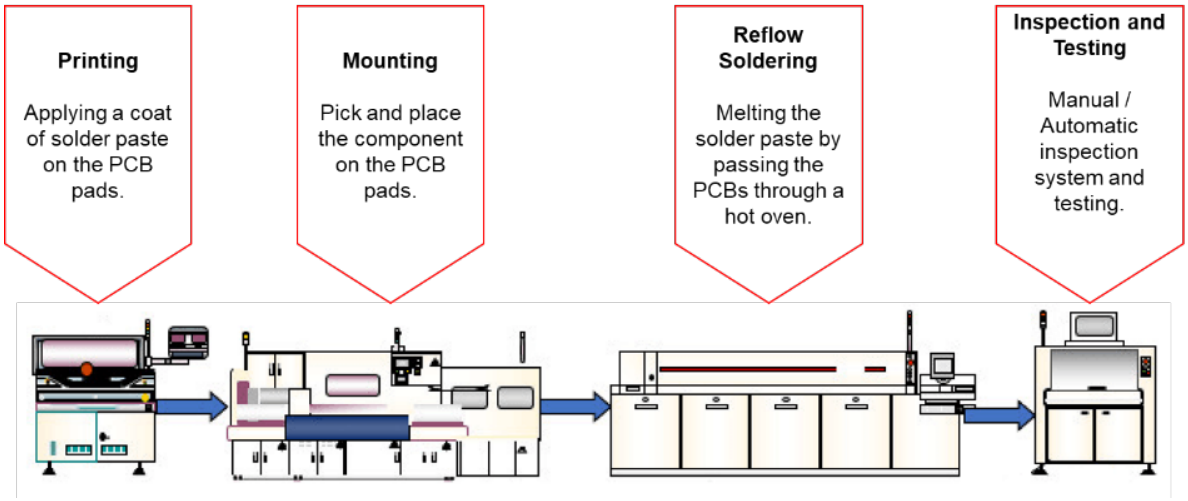


**Fig. 1** *SMT PCB manufacturing process [2]*

At the final stage, the automated inspection involves the use of computer software with AI techniques and algorithms for defects detection and classification. AXI is equipped with an X-ray source, detector, and fixture to hold and regulate the position of the component being examined. It can track different SMT devices' assembly progress defects. Contrary to Automated Optical Inspection (AOI), AXI offers more additional information that could be used to address the limitation of an optical inspection technique. The smaller size and higher density of PCBs posed a challenge for quality inspection strategies to yield an accurate inspection result. Integrating AI into automated inspection makes it feasible to precisely analyze a massive volume of data in a short period. The inspection procedure is massively improved in terms of its efficiency and effectiveness.

PCB defects detection using machine learning has been employed to design the inspection model in recent research publication [3]. These works were published in recent years. These publications include demonstrations of a wide range of machine learning techniques, focusing on deep learning and Convolutional Neural Networks (CNNs), which can identify defects in PCBs. Recently, most of the studies [4][5][6] have been focusing on the AOI technique for SMT defect detection. However, the AOI system is limited in detecting the internal layer of the PCB. Besides that, many proposed methodologies have been carried out for the PCB inspection are trained and tested confidentially. The datasets are unpublished and not available to the public [7]. Same goes to this project uses a limited private dataset from Intel, this results in difficulties of having a powerful training result as there are no extra images for expanding the data size. Therefore, this project proposed three data augmentation methods to increase the size of dataset for model training purposes, which are augmentation using Roboflow, MATLAB and a custom Generative Adversarial Network (GAN).

You-Only-Look-Once (YOLO) is a single-stage object detection algorithm that has been used in a variety of applications including PCB inspection [8][9]. It has been declared as a fast and efficient algorithm that can be used to identify and localize objects in images or video in real-time application. In [10], the author demonstrated that YOLO was able to achieve high accuracy and efficiency in detecting defects on PCBs in real-time. It uses a CNN as the backbone to extract features from images and a series of layers in the neck to fuse and enrich these features. The processed features are then fed to the head, which consists of a prediction layer that uses a classifier to predict the class of objects in the image and generate the final coordinates for the bounding boxes that surround them. Fig. 2 illustrates the structure of YOLO network.

There are many versions of YOLO model that have been published and created a big wave to the field of object detection researchers from 2015 until 2023. In this project, the YOLOv7 and YOLOv8 algorithms are introduced as the defect detection model. YOLOv7 and YOLOv8 are object detection models that were developed by K.Y.Wong [12] and Ultralytics team [13], respectively. Both algorithms use a single neural network to predict the bounding boxes and class labels of objects in an image. They are also significantly faster than previous YOLO models, making them well-suited for real-time applications.

The following objectives have been achieved at the end of this project:

1) To prepare the dataset with correct labelling and perform data augmentation techniques.
2) To detect and classify the types of defects on the tested X-ray images using proposed augmentation methods with YOLOv7 and YOLOv8 pretrained model.

Int. Journal of Integrated Engineering Vol. 16 No. 9 (2024) p. 339-350

To evaluate the performance of the proposed models in terms of the mAP scores and the accuracy of class detection in term of confusion matrix for the best proposed model.

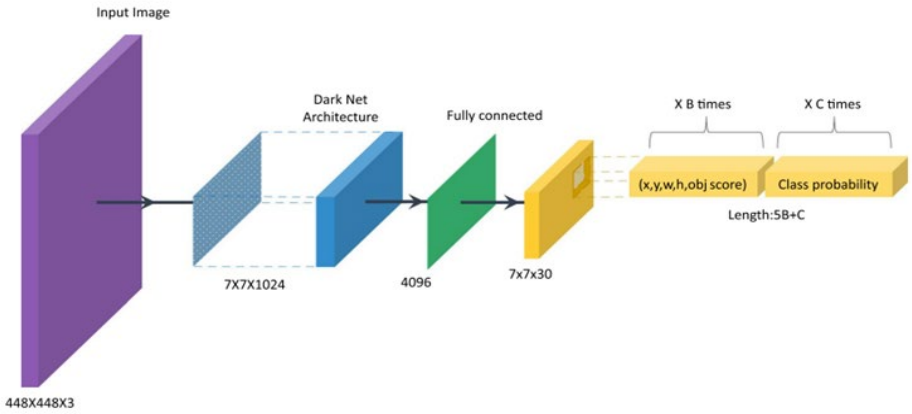


**Fig. 2** *Structure of YOLO network [11]*

## 2. Methodology

The following methods of data augmentation are introduced in the model training using selected YOLO algorithms to address the issue of handling small dataset size.

### 2.1 Data Augmentation using Roboflow (Online Method)

Roboflow serves as an online platform that offers users the capability to label and create custom datasets by providing image preprocessing and data augmentation functionalities. Various types of data augmentation techniques were applied to the original dataset, including horizontal and vertical flipping, 90° clockwise and counterclockwise rotation, flipping the image upside down, and adjusting brightness within the range of -21% to +21%. After the augmentation process, there are 329 images for training as shown in Fig. 3.

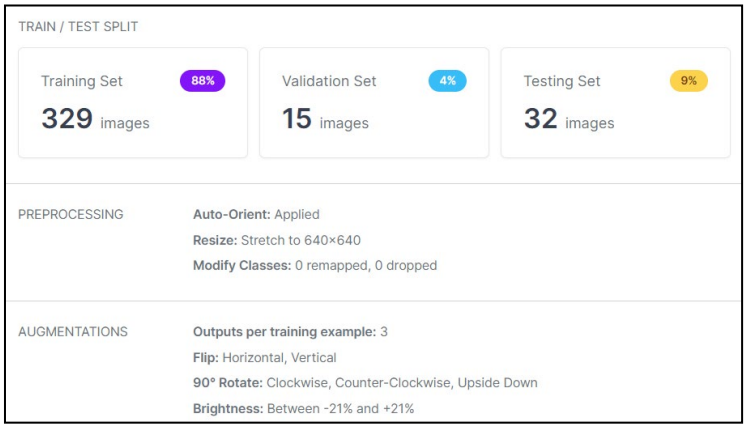


**Fig. 3** *Data augmentation in ROBOFLOW*

### 2.2 Data Augmentation using MATLAB (Offline Method)

MATLAB was used for data augmentation, such as brightness adjustment within the range of -0.1 to 0.1, contrast adjustment between 0.8 and 1.0 for grayscale images, random rotation by 90 degrees, reflection, and the addition of both salt and pepper noise, Gaussian noise, and blurred. The MATLAB training set comprised 2,300 images. Fig. 4 shows the examples of augmented images implemented in MATLAB.

### 2.3 Data Augmentation using GAN (Neural Networks Method)

GAN is a machine learning model consisting of a generator and a discriminator [14]. The generator produces synthetic data samples based on random noise, while the discriminator acts as a binary classifier distinguishing between real and fake data [15][16][17]. Through an adversarial training process, the generator learns to create increasingly realistic samples that challenge the discriminator's ability to differentiate between real and synthetic

data. This iterative training leads to the generation of high-quality synthetic data that closely resembles the real data [18][19][20]. A GAN was developed and employed to generate synthetic images based on the original dataset. By setting the number of epochs as 2,500 and saving the generated images each 100 epochs then followed by the data cleaning based on the analysis of discriminator, the total number of training data increased to 5,276 images. Fig. 5 illustrates the data augmentation process implemented in GAN.

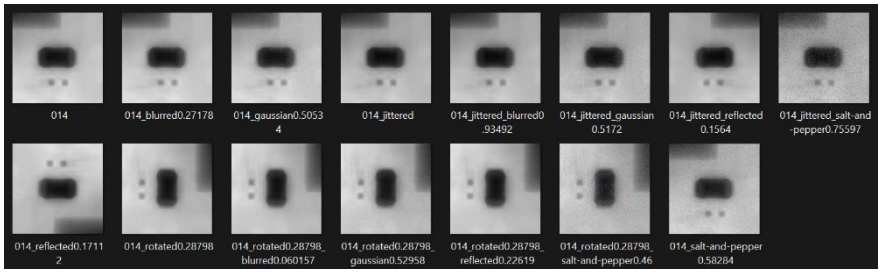


**Fig. 4** *Example of augmented images with transformations including brightness adjustments, contrast adjustments, random rotation, reflections, and the addition of salt and pepper noise, Gaussian noise, and blur effects*

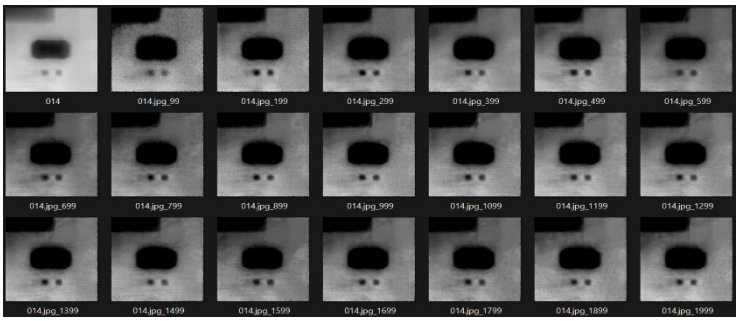


**Fig. 5** *Example of augmented images with transformations including brightness adjustments, contrast adjustments, random rotation, reflections, and the addition of salt and pepper noise, Gaussian noise, and blur effects*

## 2.4 Model Training Using YOLOv7 and YOLOv8 Models

Table 1 shows the YOLOv7 and YOLOv8 pretrained detect models based on the COCO dataset.

**Table 1** *Comparison between YOLOv7 and YOLOv8 models*

| Model | Backbones | mAP@0.5 | mAP@0.95 | Parameters (M) | Inference-Time (ms) |
|---|---|---|---|---|---|
| YOLOv7 | DarkNet-53 | 37.8 | 18.2 | 60.2 | 120 |
| YOLOv7x | DarkNet-53 | 42.9 | 22.1 | 185.0 | 240 |
| YOLOv8n | CSPDarkNet53 | 44.0 | 24.4 | 54.5 | 130 |
| YOLOv8s | CSPDarkNet53 | 43.5 | 23.4 | 21.6 | 30 |
| YOLOv8m | CSPDarkNet53 | 43.9 | 24.1 | 51.9 | 60 |

Based on the table, YOLOv8n and YOLOv8m have the highest mAP scores, and both are also the most computationally expensive model. YOLOv8s has the lowest number of parameters. Furthermore, YOLOv7x is the slowest model while YOLOv8s is the fastest then followed by YOLOv8n and YOLOv8m. Theoretically, the YOLOv8n and YOLOv8m are the best options for better accuracy whereas YOLOv8s is satisfying in terms of speed and efficiency.

## 2.5 Hyperparameters Fine-Tuning on Best Model

After obtaining the first confusion matrices of the training and evaluating result, the fine-tuning technique is taken to optimize the certain hyperparameters to improve the accuracy and performance of the model. There are three types of hyperparameters are considered, including the number of training epoch, batch size, and optimizer with learning rate. There are three sets of training that will be done to obtain the best performance based on the considered hyperparameters.

Int. Journal of Integrated Engineering Vol. 16 No. 9 (2024) p. 339-350

## 2.6 Evaluation Metrices and Expected Measurement

The evaluation on YOLOv7 and YOLOv8 models is using various data augmentation techniques. The primary evaluation metrics employed are training hours, successful training epochs, parameters, and mAP scores. Subsequently, the best-performing model, which determined based on these metrics, is further evaluated using confusion matrix to obtain the accuracy, precision, F1 score, and recall for each defect class.

## 2.7 Model Deployment

Streamlit is used for the model deployment. Streamlit web app involves making the trained model accessible through a user-friendly interface where users can interact with the model and observe its outputs. It primarily works with Python code to define the app's functionality and user interface. The trained model weight and detection python code are then imported into the web app development. It enables users to upload images, perform object detection, and view the bounding boxes on the detected SMT-Res with its classes.

## 2.8 Equipment, Tool, and Materials

Table 2 shows the equipment, tool, and materials utilized in the study.

**Table 2** *Equipment, tool, and materials used*

| Tools | Mode | Purposes |
|---|---|---|
| Roboflow | Online (Free Account) | Data labelling<br>Automated data augmentation<br>Export dataset based on YOLO requirements<br>Model deployment |
| MATLAB R2023a | Offline | Manual data augmentation<br>GAN model training<br>YOLO models evaluation |
| Google Colaboratory | Online (Free Account) | YOLO models training |

# 3. Results and Discussion

## 3.1 SMT-Res X-ray Dataset

There is a total of 200 SMT-Res defects X-ray images obtained from an AXI machine and provided by Intel's Product (M) Sdn. Bhd. All the images are in JPG format. Roboflow is used as the annotation tool for labelling the defects based on the classes, including good, missing component, solder ball, tombstone, and void. All the annotated images are then exported into YOLOv7 and YOLOv8 file format to make them accessible by the models during the training phase.

## 3.2 Model Training and Validation Results

The primary evaluation results can be found in Table 3 and Table 4. For the model training process, 100 epochs were set to prevent interruptions due to GPU limitations, while all other hyperparameters remained at their default settings.

To assess the performance of all proposed data augmentation techniques integrated with the selected YOLO pretrained models, the hyperparameters were kept constant across all models, with particular attention to the number of epochs during both the primary and secondary evaluations. By standardizing the hyperparameters to 100 epochs and a batch size of 16, as shown in Table 3 and Table 4, the YOLOv7x and YOLOv8m models achieved higher mAP@0.5 using the Roboflow-augmented dataset. However, these models required longer training times, which is time-intensive given the small dataset size. Among the models evaluated, YOLOv8n and YOLOv8s demonstrated better overall performance when considering all performance metrics. Both models achieved relatively high mean Average Precision (mAP) scores at Intersection over Union (IoU) thresholds of 0.5 and 0.95, indicating their potential in performing well with other proposed augmentation techniques.

For the MATLAB-augmented dataset, the YOLOv8m model exhibited the highest mAP scores among all the selected YOLO models. The YOLOv8n model also performed well, offering the advantage of shorter training times,

fewer parameters, and high mAP, making it particularly suited for industrial inspection tasks. YOLOv8n required only 0.71 hours for training to achieve 82.4% mAP@0.5 and 64.7% mAP@0.95 with just 3.01 million parameters.

Among the GAN-YOLO models, YOLOv8n displayed exceptional performance in terms of training time, number of parameters, and mAP scores at both IoU 0.5 and 0.95. The model completed 100 epochs of training in 2.73 hours using the largest augmented dataset and achieved impressive mAP scores of 91.1% at IoU 0.5 and 70.2% at IoU 0.95.

When comparing the MATLAB-YOLOv8n and GAN-YOLOv8n models, both delivered comparable results, meeting the requirements of Automated X-ray Inspection (AXI). YOLOv8n emerged as the superior model among all YOLOv7 and YOLOv8 variants. The slightly lower mAP@0.5 observed in the GAN-YOLOv8n model may be attributed to the larger dataset and limited number of training epochs. Despite these challenges, the GAN-YOLOv8n model showed significant potential for automated inspection, providing faster and more accurate results. Notably, the GAN-YOLOv8n model achieved a higher mAP@0.95 (70.2%) compared to the MATLAB-YOLOv8n (64.7%), which is essential for precise object detection, although it may reduce recall due to the increased accuracy demands. As seen in Table 4, all classes in GAN-YOLOv8n achieved mAP@0.5 scores above 80%.

**Table 3** *Performance metrics of proposed methods (Epoch = 100, Batch Size=16)*

| Methods | Model | Training Hours | Parameters (M) | mAP@0.5 (%) | mAP@0.95 (%) |
|---|---|---|---|---|---|
| Roboflow | YOLOv7 | 0.55 | 36.50M | 50.8 | 38.6 |
| | YOLOv7x | 0.83 | 70.81M | 76.7 | 54.7 |
| | YOLOv8n | 0.29 | 3.01M | 67.9 | 50.3 |
| | YOLOv8s | 0.29 | 11.12M | 70.8 | 56.4 |
| | YOLOv8m | 0.36 | 25.84M | 73.7 | 56.8 |
| MATLAB | YOLOv7 | 2.23 | 37.21M | 60.1 | 48.1 |
| | YOLOv7x | 2.86 | 70.84M | 80.2 | 63.1 |
| | YOLOv8n | 0.71 | 3.01M | 82.4 | 64.7 |
| | YOLOv8s | 0.79 | 11.13M | 81.0 | 63.4 |
| | YOLOv8m | 1.13 | 25.84M | 85.6 | 68.3 |
| GAN | YOLOv7 | 7.616 | 36.50M | 78.2 | 58.7 |
| | YOLOv7x | 10.44 | 70.81M | 89.0 | 67.5 |
| | YOLOv8n | 2.73 | 3.01M | 91.1 | 70.2 |
| | YOLOv8s | 3.70 | 11.13M | 85.6 | 65.7 |
| | YOLOv8m | 4.09 | 25.82M | 90.9 | 71.4 |

## 3.3 Hyperparameters Tuning

The hyperparameters chosen for model training, including the number of epochs, batch size, optimizer, and learning rate (lr), were systematically tuned. Based on the validation performance outlined in Table 5, the optimal hyperparameters were selected for each tuning set. Table 5 illustrates the class-wise evaluation of all detected classes. The optimal hyperparameters for the GAN-YOLOv8n model, as identified from Table 5, include 150 epochs, a batch size of 16, and the Adam optimizer with a learning rate of 0.001.

The confusion matrix and class-specific evaluations post-tuning are presented in Figure 6(b) and Table 6, respectively. The training and validation curves for the final 100 epochs, depicted in Figure 7, demonstrate that the model does not exhibit signs of overfitting. Both the training and validation losses decrease gradually over the epochs, indicating that the model is learning and converging appropriately. This suggests that the model is achieving a balance between learning from the training data and generalizing to new, unseen data. Concurrently, the mAP scores at IoU thresholds of 0.5 and 0.95 steadily increase over time, reflecting an improvement in object detection accuracy and localization precision. The model's performance in detecting Surface Mount Technology-Resistor (SMT-Res) defects is further evidenced by the rising mAP curve as the model learns to better identify objects and achieve higher precision and recall. Fluctuations in the curves are attributed to batch variations, learning rate adjustments, or changes in the training data.

Int. Journal of Integrated Engineering Vol. 16 No. 9 (2024) p. 339-350

Table 6 presents a comparison of class performance before and after hyperparameter tuning, with both confusion matrices displayed in Figures 6(a) and 6(b), respectively. The performance improvements following hyperparameter tuning on the GAN-YOLOv8n model, as outlined in Table 6, are evident in terms of precision, recall, mAP@0.5, and mAP@0.95. The model underwent three testing phases during training and validation, and the performance of the tuned YOLOv8n model was assessed accordingly.

Overall, the tuned YOLOv8n model outperforms the previous version, as demonstrated by the comparison in Table 7. Finally, the optimized model weights were imported into the developed Streamlit web application. The Automated X-ray Inspection (AXI) user interface, powered by the GAN-YOLOv8n model as its backend, was successfully implemented, as shown in Figure 8. By integrating GAN within the YOLOv8n architecture, the need for separate data augmentation during model training is eliminated, resulting in enhanced efficiency and significant time savings for test engineers.

**Table 4** *mAP for defect classes based on proposed methods and models (Epoch = 100, batch size=16)*

| **Methods** | **Model** | **mAP@0.5 (%)** | | | | |
|---|---|---|---|---|---|---|
| | | **Good** | **Missing Component** | **Solder Ball** | **Tombstone** | **Void** |
| Roboflow | YOLOv7 | 66.7 | 57.4 | 47.3 | 39.0 | 43.6 |
| | YOLOv7x | 63.8 | 95.5 | 95.5 | 59.4 | 65.0 |
| | YOLOv8n | 42.2 | 92.4 | 99.5 | 50.0 | 55.5 |
| | YOLOv8s | 55.4 | 86.6 | 97.2 | 67.0 | 47.7 |
| | YOLOv8m | 55.9 | 99.5 | 93.1 | 55.2 | 64.9 |
| MATLAB | YOLOv7 | 50.2 | 86.3 | 45.3 | 47.6 | 71.0 |
| | YOLOv7x | 65.1 | 99.5 | 99.6 | 69.1 | 67.5 |
| | YOLOv8n | 57.4 | 99.5 | 99.5 | 80.7 | 74.9 |
| | YOLOv8s | 59.5 | 99.5 | 99.5 | 74.3 | 72.1 |
| | YOLOv8m | 76.7 | 99.5 | 99.5 | 84.9 | 67.4 |
| GAN | YOLOv7 | 50.8 | 94.2 | 79.5 | 76.4 | 63.1 |
| | YOLOv7x | 71.4 | 97.2 | 99.6 | 77.4 | 81.1 |
| | YOLOv8n | 81.0 | 99.5 | 99.5 | 84.1 | 81.6 |
| | YOLOv8s | 78.3 | 92.7 | 99.5 | 91.6 | 74.0 |
| | YOLOv8m | 80.6 | 99.5 | 99.5 | 84.8 | 82.6 |

**Table 5** *Evaluation on GAN-YOLOv8n model after hyperparameters tuning for each set*

| **Hyperparameters** | **Variable** | **Precision (%)** | **Recall (%)** | **mAP@0.5 (%)** | **mAP@0.95 (%)** |
|---|---|---|---|---|---|
| Set 1: Epoch | 100 | 73.5 | 83.8 | 88.8 | 66.0 |
| | **150** | **85.0** | **91.7** | **92.9** | **71.5** |
| | 200 | 84.4 | 85.1 | 90.0 | 70.5 |
| Set 2: Batch | **16** | **85.0** | **91.7** | **92.9** | **71.5** |
| | 32 | 80.3 | 88.4 | 92.5 | 71.7 |
| | 64 | 83.3 | 87.5 | 91.8 | 72.2 |
| Set 3: Optimizer with its learning rate | SGD | 83.4 | 89.3 | 88.9 | 68.8 |
| | **Adam** | **85.0** | **91.7** | **92.9** | **71.5** |

**Table 6** *Classes evaluation based on confusion matrix before and after hyperparameters tuned on GAN-YOLOv8n model*

| Classes | Accuracy (%) | | Precision (%) | | Recall (%) | | F1 Score (%) | |
|---|---|---|---|---|---|---|---|---|
| Status | Before | After | Before | After | Before | After | Before | After |
| Good | 70.83 | 88.24 | 57.0 | 76.0 | 50.0 | 94.0 | 53.0 | 84.0 |
| Missing Component | 100 | 100 | 100 | 100 | 100 | 100 | 100 | 100 |
| Solder Ball | 100 | 100 | 100 | 100 | 100 | 100 | 100 | 100 |
| Tombstone | 83.33 | 96.08 | 67.0 | 100 | 86.0 | 88.0 | 75.0 | 93.0 |
| Void | 87.5 | 92.16 | 50.0 | 75.0 | 33.0 | 50.0 | 40.0 | 60.0 |

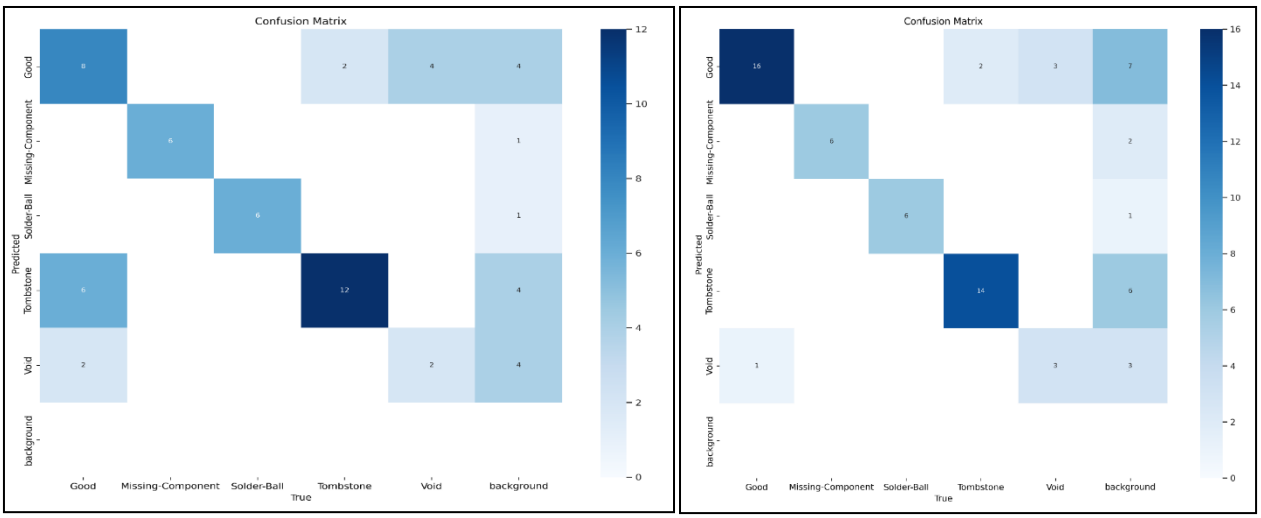


**(a)** **(b)**

**Fig. 6** *(a) Confusion matrix of GAN-YOLOv8n before tuned model; (b) Confusion matrix ofGAN-YOLOv8n after tuned model*

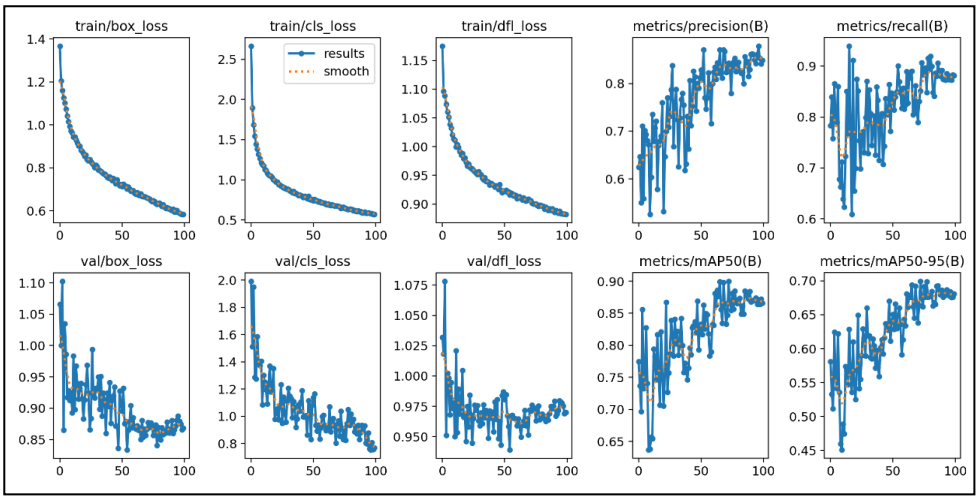


**Fig. 7** *Training and validation curves of tuned GAN-YOLOv8n model based on last 100 epochs*

Int. Journal of Integrated Engineering Vol. 16 No. 9 (2024) p. 339-350

**Table 7** *Comparison between before and after tuned GAN-YOLOv8n model*

| Classes | Accuracy (%) | Precision (%) | Recall (%) | F1 Score (%) | Accuracy in Confusion Matrix |
|---|---|---|---|---|---|
| Before | 73.4 | 89.2 | 91.1 | 70.2 | 70.83% |
| After | 85.0 | 91.7 | 92.9 | 71.5 | 88.24% |
| Differences | ↑13.65% | ↑2.73% | ↑1.98% | ↑1.85% | ↑19.73% |

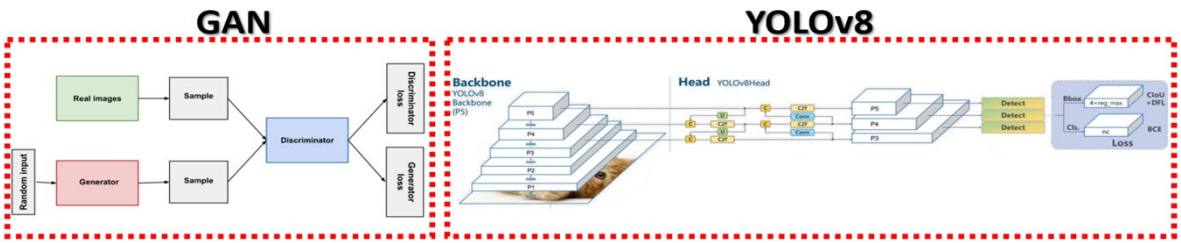


**Fig. 8** *Integration of GAN-YOLOv8 model*

## 3.4 Model Deployment

After fine-tuning the model, the weight and detect python script are then imported into Streamlit web application. It is used to configure the SMT-Res based on its class to decide either pass or fail during the inspection using AXI machine. Fig. 9 shows the GUI of the developed AXI model.

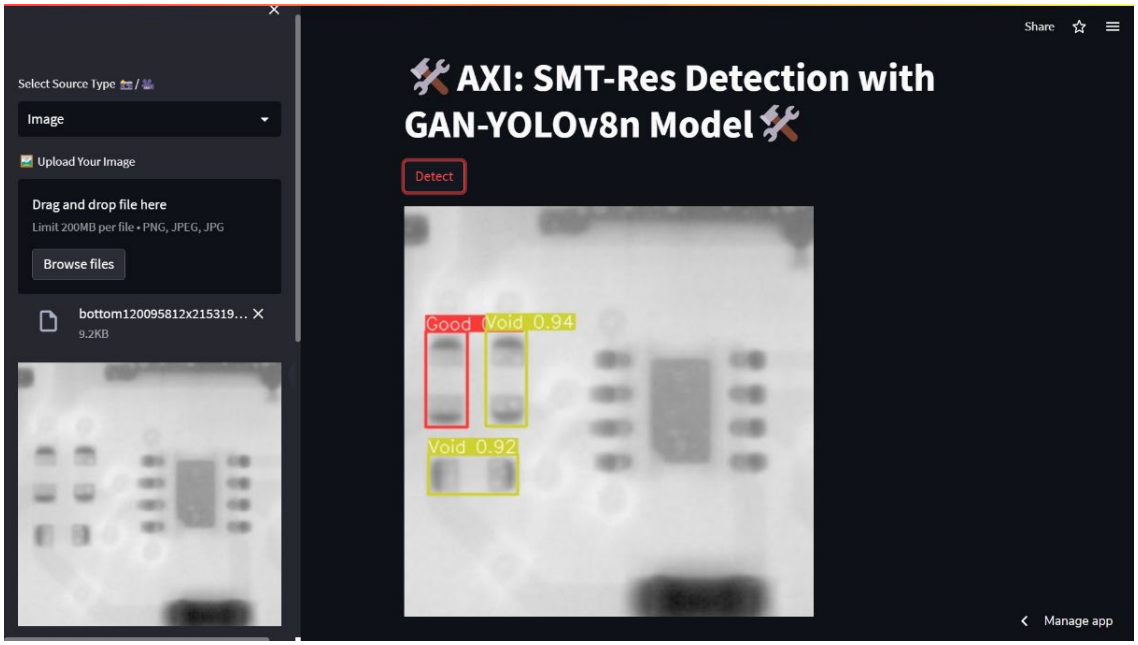


**Fig. 9** *Detection on uploaded image with bounding boxes*

## 3.5 Comparisons with Other Research Works

The comparison table (Table 8) presents a systematic evaluation of various approaches used for printed circuit board (PCB) defect detection, highlighting the methodologies and outcomes across several key studies. In the study by [21], the use of MobileNetV2 with a Feature Pyramid Network (FPN) achieved over 90% accuracy, with a mean average precision (mAP) of around 85%, suggesting that while the system demonstrated strong precision and recall, there is room for further refinement in detection tasks. Similarly, a design based on YOLOv8 by [22] reached a high defect detection accuracy of 97%, emphasizing the potential of this model for real-time manufacturing applications, but requiring improvements in scalability.

**Table 8** *Comparison with published work*

| Paper Title | Approach | Results Obtained |
|---|---|---|
| Dlamini et al., 2023 [21] | Utilizes MobileNetV2 with Feature Pyramid Network (FPN) to detect defects in surface mount devices on PCBs. Model leverages pyramid features to enhance detection. | • The defect detection system achieved an accuracy of over 90%, indicating strong performance in identifying defects on printed circuit boards.<br>• The mean average precision (mAP) was reported to be around 85%, showcasing the system's effectiveness in precision and recall for defect detection tasks.<br>• The study used 800 samples for training the defect detection system.<br>• Additionally, 200 samples were allocated for testing the system's performance. |
| Xiong, 2023 [22] | Implements YOLOv8 model for detecting defects on bare PCBs. Focuses on high-speed detection with real-time capabilities for manufacturing. | • Reached high accuracy (97%) in defect detection but did not surpass 97% in certain cases. Suggests improvements in model scalability and real-time implementation.<br>• The study utilized 800 samples for training the defect detection system.<br>• Additionally, 200 samples were used for testing the model's performance. |
| Zhang et al., 2022 [23] | Uses deep learning models to detect defects in solder joints on industrial PCBs using grayscale X-ray images. Focuses on handling varying slice numbers and ROI issues. | • Achieved high detection accuracy with reduced manual workload. Showed potential for improvement in region-of-interest (ROI) accuracy and X-ray image consistency.<br>• The results indicate that the proposed models significantly reduce the number of normal joints sent for specialist inspection, achieving a filtering rate of 73.29%.<br>• Model performance is evaluated based on Recall requirements, with specific models recommended for different thresholds (≥ 0.90 and ≥ 0.95). |
| Niu et al., 2023 [24] | Proposes an improved version of YOLOv5 with enhanced sensitivity to channel features and better handling of anchor box location for defect detection in PCBs. | • Achieved improved sensitivity to features and better accuracy. GIOU degeneration issue identified, requiring further improvement for better localization and detection.<br>• The proposed YOLOv5-based method achieved a mean average precision (mAP) of 99.1% at a speed of 86 frames per second for detecting PCB defects.<br>• The study used a total of 6720 images for training.<br>• For testing, 1067 images were utilized. |
| This article | Proposes an Automated X-ray Inspection (AXI) system that develops a defects detector framework for detecting and classifying Surface Mount Technology-Resistor (SMT-Res) on PCBs, using a private dataset from Intel Technologies. | • The YOLOv7 and YOLOv8 models are examined as detectors, and experimental results highlight the exceptional performance of the GAN-YOLOv8n model. With just 3.01M parameters, it achieves 92.9% mean average precision (mAP) at Intersection over Union (IoU) 0.5 and 71.5% mAP at IoU 0.95. |

In contrast, deep learning models applied to X-ray images in another study demonstrated their effectiveness in reducing manual workload while achieving a filtering rate of 73.29%. This approach proved particularly valuable in addressing challenges related to region-of-interest (ROI) accuracy in solder joint inspection. The study in [23] involving an improved YOLOv5 network further increased detection efficiency, achieving an impressive mAP of 99.1%, though it highlighted the need for enhancements in handling anchor box locations and addressing GIOU degeneration.

Finally, the GAN-YOLOv8n model in this study stands out for its high mAP scores of 92.9% at IoU 0.5 and 71.5% at IoU 0.95, alongside its computational efficiency with just 3.01M parameters, making it highly suitable for industrial-scale defect detection. Collectively, these studies underscore the growing potential of machine learning and deep learning techniques in improving PCB defect detection, while also identifying areas for future research, such as optimizing real-time capabilities, improving accuracy in large-scale datasets, and comparing the effectiveness of different algorithms.

## 4. Conclusions

To improve the model training, the proposed GAN-based approach, GAN-YOLOv8n, has demonstrated significant potential in overcoming dataset limitations and enhancing object detection in the context of AXI technology. GAN-YOLOv8n has demonstrated outstanding performance, which has the potential to revolutionize current AXI technology. By integrating GAN into the YOLOv8n architecture, the need for separate data augmentation during model training is eliminated, resulting in improved efficiency and time savings for test engineers. In addition, the hardware limitations pose challenges in supporting the demanding training process. Further research is needed to explore additional training epochs and establish the full potential of the GAN-YOLOv8n model. Addressing these limitations will contribute to the continued evolution of AXI technology and pave the way for enhanced object detection in electronic manufacturing sectors.

## Acknowledgement

The authors would like to thank Universiti Teknikal Malaysia Melaka (UTeM), Machine Learning and Signal Processing (MLSP) research group under the Centre for Telecommunication (CeTRI), Fakulti Teknologi dan Kejuruteraan Elektronik dan Komputer (FTKEK) for supporting this work and the use of the existing facilities to complete this study.

## Conflict of Interest

Authors declare that there is no conflict of interests regarding the publication of the paper.

## Author Contribution

*The authors are responsible for the study conception, research design, data collection, data analysis, result interpretation and manuscript drafting.*

## References

[1] Research and Markets. (2023). *Printed Circuit Board Market - Growth, Trends, COVID-19 Impact, and Forecasts* (2023-2028). Retrieved from https://www.researchandmarkets.com/reports/5275221/printed-circuit-board-market-growth-trends.

[2] Bukhari, M., Noor, N., Nan, N. M. M., & Shamsul, J. B. (2005). The application of PCB, mounted-components and solder paste in surface mount technology assembly (SMTA). In *Proceedings of the 2005 International Conference on Computer and Communication Engineering* (pp. 1-6) IEEE. https://www.researchgate.net/publication/262068141_The_Application_of_PCB_Mounted-Components_and_Solder_Paste_in_Surface_Mount_Technology_Assembly_SMTA.

[3] Ling, Q., & Isa, N. A. M. (2023). Printed circuit board defect detection methods based on image processing, machine learning and deep learning: A survey. *IEEE Access*, 11, 15921-15944. https://doi.org/10.1109/access.2023.3245093.

[4] Adibhatla, V. A., Chih, H.-C., Hsu, C.-C., Cheng, J., Abbod, M. F., & Shieh, J.-S. (2021). Applying deep learning to defect detection in printed circuit boards via a newest model of you-only-look-once. *Mathematical Biosciences and Engineering, 18(4)*, 4411-4428. https://doi.org/10.3934/mbe.2021223.

[5] Shi, W., Lu, Z., Wu, W., Liu, H., & Shi, W. (2020). Single-shot detector with enriched semantics for PCB tiny defect detection. *The Journal of Engineering*, 2020. https://doi.org/10.1049/joe.2019.1180.

[6] Shengale, R. (2021). Detection and classification of SMT defects at automated optical inspection (AOI) using residual neural network. State University of New York at Binghamton ProQuest Dissertations Publishing, 2021. 28774847.

[7] Mehta, D., True, J., Dizon-Paradis, O. P., Jessurun, N., Woodard, D. L., Asadizanjani, N., & Tehranipoor, M. (2022). Future Hardware Security Research Series 1 FICS PCB X-Ray: A Dataset For Automated Printed Circuit Board Inter-Layers Inspection. Trust-Hub. https://ia.cr/2022/924.
[8] Xie, H., Li, Y., Li, X., & He, L. (2021). A Method for Surface Defect Detection of Printed Circuit Board Based on Improved YOLOv4. *2021 IEEE 2nd International Conference on Big Data, Artificial Intelligence and Internet of Things Engineering*, ICBAIE 2021, 851-857. https://doi.org/10.1109/ICBAIE52039.2021.9390006.
[9] A. K. Lailesh, J. A. Richi and N. Preethi. A Pre-trained YOLO-v5 model and an Image Subtraction Approach for Printed Circuit Board Defect Detection. *2023 International Conference on Intelligent and Innovative Technologies in Computing, Electrical and Electronics (IITCEE)*, Bengaluru, India, 2023, pp. 140- 145. https://doi.org/10.1109/IITCEE57236.2023.10090861.
[10] Glučina, Matko, Nikola Anđelić, Ivan Lorencin, and Zlatan Car. 2023. Detection and Classification of Printed Circuit Boards Using YOLO Algorithm. Electronics 12, no. 3: 667. https://doi.org/10.3390/electronics12030667.
[11] Bhattacharya, A., & Cloutier, S. G. (2022). End-to-End Deep Learning Framework for PCB Manufacturing Defect Classification. *Scientific Reports*, 12(1). https://doi.org/10.1038/s41598-022-16302-3.
[12] Wang, Z., Wong, K. K., & Yu, Z. (2022). YOLOv7: Trainable bag-of-freebies sets new state-of-the-art for real-time object detectors. arXiv preprint arXiv:2207.02696. https://doi.org/10.48550/arXiv.2207.02696.
[13] Zhang, Z., Wang, Y., Zhang, Y., Zhang, W., & Zhang, J. (2022). Real-Time Flying Object Detection with YOLOv8. *Sensors*, 22(10), 3538. arXiv preprint arXiv:2203.15407. https://doi.org/10.48550/arXiv.2305.09972.
[14] Goodfellow, Ian J, Jean Pouget-Abadie, Mehdi Mirza, Bing Xu, David Warde-Farley, Sherjil Ozair, Aaron Courville, and Yoshua Bengio. 2014. Generative Adversarial Networks. ArXiv.org. 2014. https://doi.org/10.48550/arXiv.1406.2661
[15] You, S. (2022). PCB defect detection based on generative adversarial network. In *Proceedings of the 2022 2nd International Conference on Consumer Electronics and Computer Engineering (ICCECE)*, pp. 557-560. https://doi.org/10.1109/ICCECE54139.2022.9712737.
[16] Yang, Bokuan, yuhu nie, wenpeng cui, Jian Sun, Hao Lu, and Wei Su. Generative Adversarial Network for PCB Defect Detection with Extreme Low Compress Rate. *International Conference on Artificial Intelligence and Intelligent Information Processing (AIIIP 2022)*, 2022. https://doi.org/10.1117/12.2660551. https://doi.org/10.1117/12.2660551
[17] Wang, C., Huang, G., Huang, Z., & He, W. (2023). Conditional TransGAN-Based Data Augmentation for PCB Electronic Component Inspection. *Computational Intelligence and Neuroscience, 2023(1)*, 2024237, https://doi.org/10.1155/2023/2024237.
[18] Yumoto, S., Kitsukawa, T., Moro, A., Pathak, S., Nakamura, T., & Umeda, K. (2023). Anomaly detection from images in pipes using GAN. *ROBOMECH Journal, 10(1)*. https://doi.org/10.1186/s40648-023-00246-y.
[19] A. Yang, C. Lu, W. Yu, J. Hu, Y. Nakanishi and M. Wu. (2023). Data Augmentation Considering Distribution Discrepancy for Fault Diagnosis of Drilling Process with Limited Samples. *IEEE Transactions on Industrial Electronics, vol. 70, no. 11*, pp. 11774-11783, Nov. 2023. https://doi.org/10.1109/TIE.2022.3229274.
[20] Yu, Xinyi, and Yuanfu He. PCB Defect Detection Based on GAN Data Generation with Self-Attentive Mechanism. *2022 2nd International Conference on Frontiers of Electronics, Information and Computation Technologies (ICFEICT)*, 1 Aug. 2022, https://doi.org/10.1109/icfeict57213.2022.00018.
[21] Dlamini, S., Kuo, C.-F. J., & Chao, S.-M. (2023). Developing a surface mount technology defect detection system for mounted devices on printed circuit boards using a MobileNetV2 with Feature Pyramid Network. *Engineering Applications of Artificial Intelligence*, 121, 105875. https://doi.org/10.1016/j.engappai.2023.105875
[22] Niu, J., Li, H., Chen, X., & Qian, K. (2023). An Improved YOLOv5 Network for Detection of Printed Circuit Board Defects. *Journal of Sensors*, 2023(1). https://doi.org/10.1155/2023/7270093
[23] Xiong, Z. (2023). A Design of Bare Printed Circuit Board Defect Detection System Based on YOLOv8. *Highlights in Science, Engineering and Technology*, 57, 203–209. https://doi.org/10.54097/hset.v57i.10002
[24] Zhang, Q., Zhang, M., Gamanayake, C., Yuen, C., Geng, Z., Jayasekara, H., Woo, C., Low, J., Liu, X., & Guan, Y. L. (2022). Deep learning based solder joint defect detection on industrial printed circuit board X-ray images. *Complex & Intelligent Systems, 8(2)*, 1525–1537. https://doi.org/10.1007/s40747-021-00600-w